

Local Distance Functions: A Taxonomy, New Algorithms, and an Evaluation

Deva Ramanan and Simon Baker

Deva Ramanan is with UC Irvine.

Simon Baker is with Microsoft Research.

A preliminary version of this paper appeared in the IEEE International Conference on Computer Vision [32].

Abstract

We present a taxonomy for local distance functions where most existing algorithms can be regarded as approximations of the geodesic distance defined by a metric tensor. We categorize existing algorithms by **how**, **where**, and **when** they estimate the metric tensor. We also extend the taxonomy along each axis. **How**: We introduce hybrid algorithms that use a combination of techniques to ameliorate overfitting. **Where**: We present an exact polynomial time algorithm to integrate the metric tensor along the lines between the test and training points under the assumption that the metric tensor is piecewise constant. **When**: We propose an interpolation algorithm where the metric tensor is sampled at a number of reference points during the offline phase. The reference points are then interpolated during the online classification phase. We also present a comprehensive evaluation on tasks in face recognition, object recognition, and digit recognition.

Index Terms

Nearest Neighbor Classification, Metric Learning, Metric Tensor, Local Distance Functions, Taxonomy, Database, Evaluation

I. INTRODUCTION

The K-nearest neighbor (K-NN) algorithm is a simple but effective tool for classification. It is well suited for multi-class problems with large amounts of training data, which are relatively common in computer vision. Despite its simplicity, K-NN and its variants are competitive with the state-of-the-art on various vision benchmarks [6], [23], [43].

A key component in K-NN is the choice of the distance function or metric. The distance function captures the type of invariances used for measuring similarity between pairs of examples. The simplest approach is to use a Euclidean distance or a Mahalanobis distance [14]. Recently, a number of approaches have tried to learn a distance function from training data [5], [15], [23], [24], [38]. Another approach is to define a distance function analytically based on high level reasoning about invariances in the data. An example is the tangent distance [37].

The optimal distance function for 1-NN is the probability that the pair of examples belong to different classes [28]. The resulting function can be quite complex, and generally can be expected to vary across the space of examples. For those motivated by psychophysical studies, there is also evidence that humans define categorical boundaries in terms of local relationships between exemplars [34]. The last few years have seen an increased interest in such local distance functions

TABLE I

A SUMMARY OF OUR TAXONOMY FOR LOCAL DISTANCE FUNCTIONS. ALGORITHMS CAN BE CLASSIFIED BY **how**, **when**, AND **where** THEY ESTIMATE THE METRIC TENSOR. WE ALSO PROPOSE A NUMBER OF EXTENSIONS TO THE TAXONOMY (MARKED IN **bold**.)

		Where				
		Whole Space	Each Class	Training Points	Test Point	Line Integral
How		Dim. Reduction/LDA				
		Metric Learning				
		Hybrid (Sec. II-B.3)				
When	Offline	Global	Per-Class	Small DB Only	N/A	N/A
	Online	As Above	As Above	Per-Exemplar	Lazy	Too Slow
	Interp.	As Above	As Above	Sec. II-D.3	Sec. II-D.3	Sec. II-E

for nearest neighbor classification [12], [13], [30], [43], though similar ideas were explored earlier in the context of local discriminant analysis [10], [19] and locally weighted learning [3], [35]. Recent approaches have also leveraged local metrics for Gaussian process regression [39] and multiple kernel learning [16].

Our first contribution is to present a taxonomy for local distance functions. In particular, we show how most existing algorithms can be regarded as approximations of the geodesic distance defined by a metric tensor. We categorize existing algorithms in terms of **how**, **where**, and **when** they estimate the metric tensor. See Table I for a summary. In terms of **how**, most existing algorithms obtain a metric either by dimensionality reduction such as principle components analysis (PCA) or linear discriminant analysis (LDA) [14], or by explicit metric-learning [5], [15], [24]. In terms of **where**, existing algorithms sample the metric tensor: (a) for the whole space (“global”), (b) for each class (“per-class”) [24], (c) at the training points (“per-exemplar”) [12], [13], or (d) at the test point [3], [19]. In terms of **when**, existing algorithms either estimate the metric tensor: (a) offline during training or (b) online during classification.

Our second contribution is to extend the taxonomy along each dimension. In terms of **how**, we introduce hybrid algorithms that use a combination of dimensionality reduction and metric learning to ameliorate over-fitting. In terms of **where**, we consider algorithms to integrate the

metric tensor along the line between the test point and the training point. We present an exact polynomial time algorithm to compute the integral under the assumption that the metric tensor is piecewise constant. In terms of **when**, we consider a combined online-offline algorithm. In the offline training phase, a representation of the metric tensor is estimated by sampling it at a number of reference points. In the online phase, the metric tensor is estimated by interpolating the samples at the reference points.

Our third contribution is to present a comprehensive evaluation of the algorithms in our framework, both prior and new. We show results on a diverse set of problems, including face recognition using MultiPIE [18], object recognition using Caltech 101 [11], and digit recognition using MNIST [27]. To spur further progress in this area and allow other researchers to compare their results with ours, we will make the raw feature vectors, class membership data, and training-test partitions of the data available on a website with the goal of defining a standard benchmark¹.

II. TAXONOMY AND ALGORITHMS

We now present our framework for local distance functions. We begin in Section II-A by describing the scenario and class of functions that we consider. We introduce the metric tensor and explain how it defines the geodesic distance. In Section II-B we describe how the core distance functions can be learnt using either dimensionality reduction or metric learning and extend the framework to include hybrid algorithms. In Section II-C we describe how several well-known local distance functions can be viewed as approximations to the geodesic distance by sampling the metric tensor at the appropriate point(s). In Section II-C we only consider algorithms that can (at least conceptually) be applied before the test point is known. In Section II-D we consider the time at which the metric tensor is estimated or sampled. Besides offline algorithms, we consider online algorithms that require the test point to be known before they can be applied. We also extend the framework to algorithms that first estimate the metric tensor at a number of reference points and then interpolate them during online classification. In Section II-E we present a polynomial time algorithm to integrate the metric tensor along the lines between the test and training points.

¹Available at <http://www.ics.uci.edu/~dramanan/localdist/>

A. Background

1) *Problem Scenario:* We assume that we are working with a classification problem defined in a K dimensional feature space R^K . Each test sample is mapped into this space by computing a number of features to give a point $\mathbf{x} \in R^K$. Similarly, each training sample is mapped into this space to give a point $\mathbf{x}_i \in R^K$. Where appropriate, we denote the test point by \mathbf{x} and the training points by \mathbf{x}_i . We do not consider problems where all that can be computed is the pairwise distance or kernel matrix between each pair of test and training sample $\text{Dist}(\mathbf{x}, \mathbf{x}_i)$. A number of learning algorithms have been proposed for this more general setting [12], [13]. Note, however, that such general metrics often measure the distance between two images under some correspondence of local features and that approximate correspondence can be captured by a pyramid vector representation [17]. An important alternate class of models define similarity using a kernel function or weighted combination of kernel functions [4], [9], [21], [40]. Mercer's theorem guarantees that kernels implicitly embed data points in a feature space [9]. This feature space is typically finite dimensional. Example kernels commonly used in image matching include the intersection kernel and pyramid match kernel [17], [17], [29]. Notable exceptions include the Gaussian kernel. Many, if not most, distance functions either explicitly or implicitly embed data in a finite dimensional vector space. Our work applies to this common case.

2) *Set of Distance Functions Considered:* We consider distance functions that can be written in the form:

$$\text{Dist}_M(\mathbf{x}, \mathbf{x}_i) = (\mathbf{x}_i - \mathbf{x})^T M (\mathbf{x}_i - \mathbf{x}). \quad (1)$$

where M is a $K \times K$ symmetric, positive definite matrix. The set of functions defined by Equation (1) are metrics. In this paper, we interchangeably refer to the functions of the form in Equation (1) and the matrices M as metrics, even though not all metrics can be written in that form. Most existing algorithms, with the notable exceptions of [12], [13], consider the set of metrics in Equation (1), or a subset of them. In many cases the positive definite condition is relaxed to just non-negativity in which case, strictly speaking M is a psuedometric. In other cases, only diagonal M are considered.

3) *The Metric Tensor:* The metric tensor is a generalization of a single constant metric of the form in Equation (1) to a possibly different metric at each point in the space [1], [2]. The most common use of the metric tensor is to define distances on a manifold. In our case the

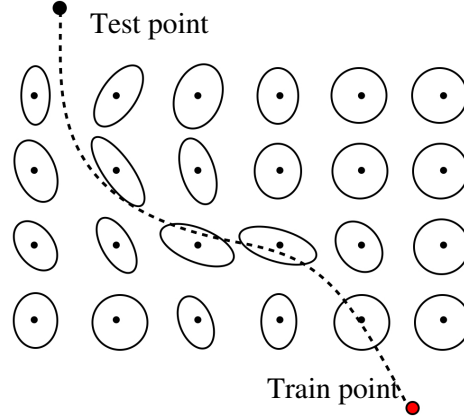


Fig. 1. An illustration of the geodesic distance defined by a metric tensor. We visualize metrics sampled at grid points in R^2 by displaying the isocontour of equivalent distances. The length of a particular path between the red and black points is computed by integrating the metric tensor along the path. The geodesic distance is the minimum length path, over all such paths. The shortest path is shown as the dotted curve above.

manifold is R^K which has a global coordinate system. We therefore do not need to worry about the coordinate transforms between the tensor representations, but instead can represent it as a single matrix $MT(\mathbf{x})$ at each point \mathbf{x} in the space. Roughly speaking, $MT(\mathbf{x})$ can be thought of as defining a local distance function or metric $\text{Dist}_{MT(\mathbf{x})}$ at each point in the space.

4) *Geodesic Distance*: Given a piecewise differentiable curve $\mathbf{c}(\lambda)$, where $\lambda \in [0, 1]$, the length of the curve is given by:

$$\text{Length}(\mathbf{c}(\lambda)) = \int_0^1 \left[\frac{d\mathbf{c}}{d\lambda} \right]^T MT(\mathbf{c}(\lambda)) \frac{d\mathbf{c}}{d\lambda} d\lambda. \quad (2)$$

The geodesic distance between a pair of test and training points is the distance of the shortest curve between them:

$$\text{Dist}_{\text{Geo}}(\mathbf{x}, \mathbf{x}_i) = \min_{\mathbf{c}(0)=\mathbf{x}, \mathbf{c}(1)=\mathbf{x}_i} \text{Length}(\mathbf{c}(\lambda)). \quad (3)$$

In Figure 1 we illustrate the metric tensor and the geodesic distance between a test point and a training point. We visualize the metrics sampled at grid points by displaying the isocontour of equivalent distances, which in R^2 are ellipses. The shortest path between two points is not necessarily the straight line between them, but in general is curved.

If the metric tensor is (close to) zero within each class, and has a large non-zero component across the boundary of each class, then theoretically perfect classification can be obtained in the

absence of noise using the geodesic distance and just a single training sample in each connected component of each class. Estimating such an ideal metric tensor would require a very dense sampling of training data, in which case classification using nearest neighbors and a Euclidean metric would work well. But at heart, we argue that all local distance function algorithms are based on the hope that better classification can be obtained for typical training data densities by using a spatially varying metric tensor and an approximation to the geodesic distance.

We now introduce our taxonomy and describe the possible choices for a local distance function-based algorithm in terms of **how**, **when**, and **where** it estimates the metric tensor and approximates the geodesic distance. We demonstrate that the interpretation of local distance functions as approximating geodesics allows for a unification of many approaches under a general taxonomy, as well as suggesting new algorithms.

B. How

The first component in our taxonomy is **how** the metric tensor is estimated at any given point (or region) in the space in terms of a number of training samples close to that point.

1) *Dimensionality Reduction Algorithms*: Perhaps the simplest metric learning algorithms are the various linear dimensionality reduction algorithms. For example, Principle Components Analysis (PCA) [14] projects the data into a low-dimensional subspace and then measures distance in the projected space. If P is the (orthonormal) $d \times K$ dimensional PCA projection matrix, the corresponding distance between a pair of test and training points:

$$\|P(\mathbf{x}_i - \mathbf{x})\|^2 = (\mathbf{x}_i - \mathbf{x})^T M_{\text{PCA}}(\mathbf{x}_i - \mathbf{x}) \quad (4)$$

where $M_{\text{PCA}} = P^T P$ is the corresponding metric. Rather than an explicit projection, one can use a Mahalanobis distance [14] (the inverse of the sample covariance matrix.)

A more powerful approach is to learn a subspace that preserves the variance between class labels using Linear Discriminant Analysis (LDA) [14]. LDA has a large number of variants. In this paper we consider a weighted form of **Regularized LDA** [14] described below. We assume we are given a set of triples $\{x_i, y_i, w_i\}$ consisting of data points, class labels, and weights. We can interpret integer weights as specifying the number of times an example appears in an equivalent unweighted dataset. We search for the $d \times K$ dimensional LDA basis V that

maximizes:

$$\begin{aligned} \arg \max_V \operatorname{tr}(V^T \Sigma_B V) \quad \text{s.t.} \quad V^T (\Sigma_W + \lambda I) V = I & \quad \text{(LDA)} \\ \Sigma_B = \frac{1}{C} \sum_j \bar{\mu}_j \bar{\mu}_j^T, \quad \Sigma_W = \frac{\sum_i w_i \bar{x}_i \bar{x}_i^T}{\sum_i w_i}, \quad \bar{x}_i = x_i - \mu_{y_i} \\ \bar{\mu}_j = \mu_j - \frac{1}{C} \sum_j \mu_j, \quad \mu_j = \frac{\sum_{\{i:y_i=j\}} w_i x_i}{\sum_{\{i:y_i=j\}} w_i} \end{aligned}$$

where C is the number of classes. This can be solved with a generalized eigenvalue problem. Because the rank of Σ_B is upper bounded by C and generally $C < K$ we use a bagged estimate of Σ_B obtained by averaging together covariance matrices estimated from sub-sampled data [42]. The regularization parameter λ enforces an isotropic Gaussian prior on Σ_W that ensures that the eigenvalue problem is well conditioned when Σ_W is low rank. We found this explicit regularization was essential for good performance even when Σ_W is full rank. We used a fixed $\lambda = 1$ for all our experiments.

As defined in Equation (LDA), V is not guaranteed to be orthonormal. We explicitly apply Gram-Schmidt orthonormalization to compute V_G and define the LDA metric: $M_{\text{LDA}} = V_G^T V_G$ where M_{LDA} is a $K \times K$ matrix of rank d . An alternative approach [19] is to use the scatter matrices directly to define a full-rank metric $M = S_W^{-1} S_B S_W^{-1}$. Empirically, we found the low-rank metric M_{LDA} to perform slightly better, presumably due to increased regularization.

2) *Metric Learning Algorithms*: Recently, many approaches have investigated the problem of learning a metric M that minimizes an approximate K-NN error on a training set of data and class label pairs $\{x_i, y_i\}$ [5], [15], [23], [24], [38]. Relevant Component Analysis (RCA) [5] finds the basis V that maximizes the mutual information between x_i and its projection Vx_i while requiring that that distances between projected points from the same class remain small. Neighborhood Component Analysis (NCA) [15] minimizes a probabilistic approximation of the leave-one-out cross validation error. Recent approaches minimize a hinge-loss approximation of the misclassification error [23], [24], [38].

The state-of-the-art at the time of writing appears to be the Large Margin Nearest Neighbor (LMNN) algorithm [24]. LMNN defines a loss function L that penalizes large distances between “target” points that are from the same class while enforcing the constraint that, for each point i , “imposter” points k from different classes are 1 unit further away than target neighbors j . We

define a generalization that uses a weighted error similar to (**LDA**):

$$L(M) = \sum_{\{ij\} \in Targ} w_i \text{Dist}_M(\mathbf{x}_i, \mathbf{x}_j) + \tag{LMNN} \\ C \sum_{\{ijk\} \in Imp} w_i h(\text{Dist}_M(\mathbf{x}_i, \mathbf{x}_k) - \text{Dist}_M(\mathbf{x}_i, \mathbf{x}_j)).$$

The constraint is enforced softly with a hinge loss function h , making the overall objective function convex. It can be solved with a semi-definite program (SDP). We used publicly available LMNN code [24] in our experiments.

One limitation of the above approach is that an initial (Euclidean) metric must be used to define the target and imposter neighbors. One might imagine an iterative procedure in which the newly learned LMNN-metric is used to define new target/imposter neighbors for a subsequent LMNN-learned metric. Weinberger and Saul investigate such a multi-pass LMNN algorithm [24], but observe that it tends to overfit for small-sized training data. As such, we do not pursue it in our analysis.

3) *New Algorithm: Hybrid Approach:* Some local distance function algorithms invoke multiple metrics at various stages. For example, many local algorithms require an initial global metric to produce a *short list* of candidate training points which are then processed by a more expensive local metric. See Section III-A.1 for more details. More generally in our taxonomy below, many local algorithms use a global metric to determine **where** in the space to estimate the local approximation to the metric tensor.

The metric learning algorithm need not be the same in the two stages. In this paper we consider a hybrid approach where different metric learning algorithms are used in the two steps. Specifically, we use LMNN to decide where to estimate the metric tensor and populate a short list, and Regularized LDA to estimate the local metric. The local estimation of a metric is more dependent on regularization. Empirically we found LMNN to be more powerful when supplied with ample training data and LDA to be far easier to regularize when estimating a local metric. Note that Hybrid learning does not apply for the Global setting in our taxonomy, as only a single metric is learned.

C. *Where: Offline Algorithms*

We now begin to study the **where** dimension of our taxonomy. In this section we only consider algorithms that can be applied before the test point is known. Sections II-D.2 (Lazy) and II-

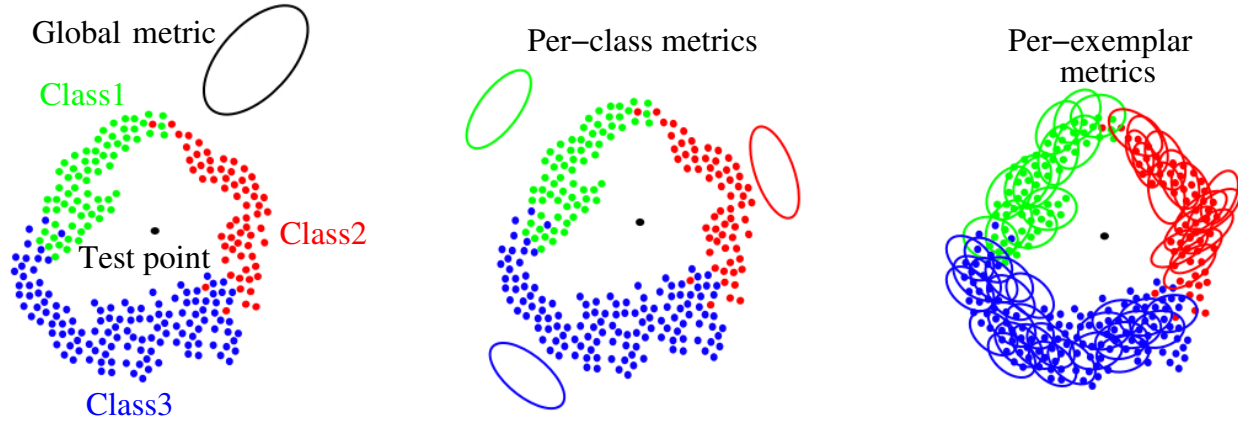


Fig. 2. An illustration of the “where” dimension of our taxonomy. Besides using a single global metric, a separate metric can be used for each class (“per-class”) or for each training example (“per-exemplar”). In this figure and in Section II-C we restrict attention to algorithms that can be applied before the test point is known. In Section II-D.2 we consider algorithms that estimate the metric tensor at the test point and in Section II-E we described an algorithm that integrates the metric tensor along the lines between the test point and the training points.

E (Line Integral) describe other options in the where dimension. We illustrate the algorithms considered in this section in Figure 2.

1) *Over the Whole Space: Global:* The baseline approach is to assume that the metric tensor is constant throughout the space and compute a single **Global** metric for the whole space using all of the training data $MT(\mathbf{x}) = M_{\text{Global}}$. If the metric tensor is a constant, then the shortest path geodesic distance in Equation (3) is the distance along the direct path $\mathbf{c}(\lambda) = \mathbf{x} + \lambda(\mathbf{x}_i - \mathbf{x})$ between the points which simplifies to:

$$\text{Dist}_{\text{Global}}(\mathbf{x}, \mathbf{x}_i) = (\mathbf{x}_i - \mathbf{x})^T M_{\text{Global}} (\mathbf{x}_i - \mathbf{x}). \quad (5)$$

2) *For Each Class: Per-Class:* Another alternative is to approximate the metric tensor with a constant metric for each class, commonly referred to as a **Per-Class** metric [24]:

$$MT(\mathbf{x}_i) = M_{\text{Per-Class}}^j \quad \text{where } j = \text{Class}(\mathbf{x}_i). \quad (6)$$

In particular, there is a different metric M_{PerClass}^j for each class j . One simple approach to learn M_{PerClass}^j is to optimize the weighted score from (**LDA**) or (**LMNN**) where $w_i = 1$ for $\{i : y_i = j\}$ and 0 otherwise. When computing the distance from a test point \mathbf{x} to a training point \mathbf{x}_i we assume the metric tensor is constant along all paths from \mathbf{x} to \mathbf{x}_i :

$$\text{Dist}_{\text{PC}}(\mathbf{x}, \mathbf{x}_i) = (\mathbf{x}_i - \mathbf{x})^T M_{\text{Per-Class}}^{\text{Class}(\mathbf{x}_i)} (\mathbf{x}_i - \mathbf{x}). \quad (7)$$

Generally speaking, metrics learned for each class may not be comparable, since they are trained independently. Similar issues arise in multiclass learning because multiple one-versus-all classifiers may not be directly comparable, although in practice, such a strategy is often employed [33]. We make LDA metrics comparable by normalizing each to have a unit trace. We fix the rank d of the LDA metric to be the number of distinct classes present among the neighbors of the training examples of class j . To normalize the LMNN metrics, we follow the approach introduced in [13] and [24] and define a generalization of Equation (LMNN) that learns metrics M_c for all the classes together:

$$L(\{M_c\}) = \sum_{\{ij\} \in \text{Targ}} \text{Dist}_{M_{y_i}}(\mathbf{x}_i, \mathbf{x}_j) + \quad (8)$$

$$C \sum_{\{ijk\} \in \text{Imp}} h(\text{Dist}_{M_{y_i}}(\mathbf{x}_i, \mathbf{x}_k) - \text{Dist}_{M_{y_i}}(\mathbf{x}_i, \mathbf{x}_j)).$$

3) *At the Training Points: Per-Exemplar:* Another approximation is to assume that the metric tensor is constant within the neighborhood of each training sample \mathbf{x}_i and use a **Per-Exemplar** metric:

$$MT(\mathbf{x}) = M_{\text{Per-Exemplar}}^{\mathbf{x}_i} \quad (9)$$

for points \mathbf{x} close to \mathbf{x}_i . An example of the Per-Exemplar approach, used in a more general non-metric distance function, is [12], [13]. A simple approach to learn $M_{\text{Per-Exemplar}}^{\mathbf{x}_i}$ is to optimize Equation (LDA) or (LMNN) with neighboring points weighted by one ($w_i = 1$) and far away points are weighted by ($w_i = 0$). As in LMNN, an initial metric must be used to construct these neighbors. We found that a global metric, learned with either LDA or LMNN (as dictated by the ‘‘How’’ taxonomy criterion), outperformed a Euclidean metric for the purposes of identifying neighbors.

Again, these local metrics may not be comparable. As before, we trace-normalize the LDA metrics. In theory, one can define an extension of Equation (8) that simultaneously learns all LMNN exemplar metrics. This is infeasible due to the number on training exemplars, and so we independently learn LMNN exemplar metrics. In practice, this still performs well because the initial pruning step (creating a shortlist) tends to select close-by exemplars whose metrics are learned with similar data.

When computing the distance from a test point \mathbf{x} to a training point \mathbf{x}_i we assume the metric tensor is constant along all paths from \mathbf{x} to \mathbf{x}_i and so use the metric of \mathbf{x}_i :

$$\text{Dist}_{\text{PE}}(\mathbf{x}, \mathbf{x}_i) = (\mathbf{x}_i - \mathbf{x})^T M_{\text{Per-Exemplar}}^{\mathbf{x}_i} (\mathbf{x}_i - \mathbf{x}). \quad (10)$$

D. When

We now consider the **when** dimension of our taxonomy. We first consider traditional algorithms, both offline and online. Afterwards we present an interpolation algorithm which estimates the metric tensor at a number of reference points in an offline phase and then interpolates these estimates in the online classification phase.

1) *Offline*: Offline algorithms compute the metric at train time, before any test points are given. In Table I only the **Global**, **Per-Class** and **Per-Exemplar** algorithms could be used offline. The **Lazy** and **Line Integral** approaches require the test point and so cannot be applied. The Global approach is the most common [5], [15], [23], [24], [38], and also the least computationally demanding. Given a dataset with M training points in C classes in a K dimensional space, just a single metric must be estimated and the storage requirement is only $O(K^2)$. The Per-Class approach [24] must estimate C metrics, and so requires storing $O(CK^2)$. A non-metric variant of the Per-Exemplar approach has also been used in the past [12], [13]. Since the number of training points M is typically much larger than the number of classes, the storage cost $O(MK^2)$ can make the application of this approach in an offline fashion intractable for very large datasets including ours. One can, however, define an ‘‘online’’ Per-Exemplar that first computes a short-list of exemplars for a test point using a global metric. One can then learn metrics of each short-listed exemplar on-the-fly, use them to re-rank the exemplars, and discard them without any need for storage. We include this algorithm in our experiments.

2) *Online at the Test Point: Lazy*: Once the test point has been provided during the online classification phase, another option is to estimate the metric tensor at the test point:

$$MT(\mathbf{x}) = M_{\text{Lazy}}^{\mathbf{x}}. \quad (11)$$

See Figure 3(left) for an illustration. This approach requires learning the metric at run time which is why we refer to it as **Lazy**. The training set for the Lazy algorithm consists of S training points \mathbf{x}_i close to the test point \mathbf{x} . In our experiments, we use a Global metric to define which points are the closest and set $S = 50$. We set w_i for these training points to be 1 and

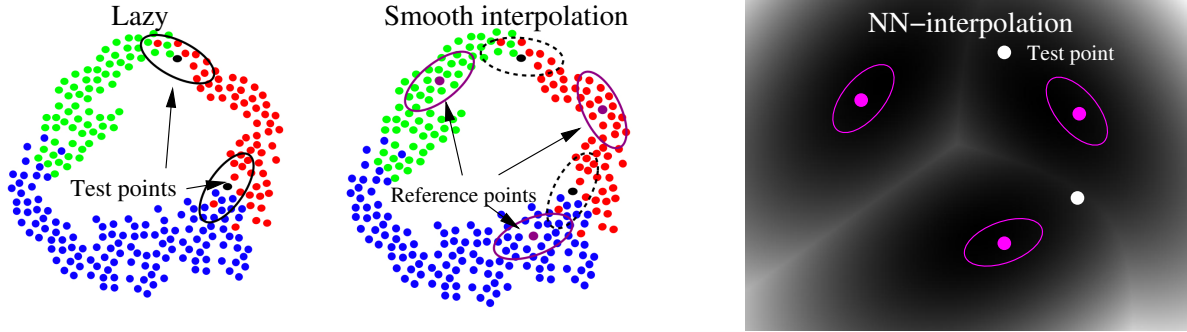


Fig. 3. An illustration of the “when” dimension of our taxonomy. **Left:** The **Lazy** algorithm estimates the metric tensor at the test point, which shifts the computation online. An obvious drawback of the Lazy approach is the computational cost. **Middle:** Our interpolation algorithm precomputes the metric tensor at a small subset of reference points. The online metric is computed by interpolating the metrics at the reference points. We describe two approaches using radial basis functions (**Middle**) and simple NN-interpolation. With proper construction of the reference metrics, NN-interpolation can perform similarly to Lazy with a reduction in computational cost. **Right:** NN-interpolation carves up the vector space into an anisotropic Voronoi diagram with quadratic boundaries between Voronoi cells [25].

0 otherwise, and optimize Equation (**LDA**) or (**LMNN**) to learn $M_{\text{Lazy}}^{\mathbf{x}}$. We fix the rank d of the LDA metric to the number of distinct classes present in the S training neighbors. When computing the distance from a test point \mathbf{x} to a training point \mathbf{x}_i we assume the metric tensor is constant along all paths from \mathbf{x} to \mathbf{x}_i and use the metric estimated at the test point \mathbf{x} :

$$\text{Dist}_{\text{Lazy}}(\mathbf{x}, \mathbf{x}_i) = (\mathbf{x}_i - \mathbf{x})^T M_{\text{Lazy}}^{\mathbf{x}} (\mathbf{x}_i - \mathbf{x}). \quad (12)$$

Examples of the **Lazy** algorithm are the local discriminant adaptive algorithm of [19], the locally weighted learning algorithm of [3], and the locally adaptive metric algorithm of [10]. These algorithms all use a global metric to select the S nearest neighbors of a test point \mathbf{x} which are then classified using a locally learnt distance function. Zhang et al [43] use a similar approach, but directly learn a local discriminant boundary using an SVM rather than learning a local metric.

3) *New Algorithms: Interpolation:* We expect the metric tensor $MT(\mathbf{x})$ to vary smoothly. This suggests that we can interpolate the metric tensor from a sparse set of samples. Assume that a subset of the training examples has been selected. We refer to these points \mathbf{x}_{RP_i} for $i = 1, \dots, R$ as reference points. We use radial basis function interpolation to interpolate the metric tensor in the remaining parts of the space [7]. In our experiments we chose the reference points at

random, however, a more principled approach to distribute the reference points uniformly could have been used.

Offline, local metrics $M_{RP}^{\mathbf{x}_{RP}^i}$ are computed for the reference points by optimizing Equation (LDA) or (LMNN) with $w_{RP_i} = 1$ and 0 otherwise. One could learn these metrics jointly but we found independently learning the metrics sufficed. Online, the local metrics $M_{RP}^{\mathbf{x}_{RP}^i}$ are interpolated to obtain the final metric. One approach is nearest neighbor (NN) interpolation:

$$MT_{NN}(\mathbf{x}) = M_{RP}^{\mathbf{x}_{RP}^i} \quad \text{where} \quad i = \underset{j}{\operatorname{argmin}} \operatorname{Dist}_{\text{Global}}(\mathbf{x}, \mathbf{x}_{RP_j}). \quad (13)$$

Here we use a Global metric to define closeness to the references points. Another approach would be to use that reference point's own metric, as is done in Section II-E. We saw similar performance in either case with a slight speed up with Global. Another approach would be to use a smooth weighted average of the metrics obtained through radial basis function (RBF) interpolation [7]:

$$MT_{RBF}(\mathbf{x}) = \sum_{i=1}^R w_i(\mathbf{x}) M_{RP}^{\mathbf{x}_{RP}^i} \quad (14)$$

$$w_i(\mathbf{x}) = \frac{e^{-\frac{1}{\sigma} \operatorname{Dist}_{\text{Global}}(\mathbf{x}, \mathbf{x}_{RP}^i)}}{\sum_{j=1}^R e^{-\frac{1}{\sigma} \operatorname{Dist}_{\text{Global}}(\mathbf{x}, \mathbf{x}_{RP}^j)}}. \quad (15)$$

In our experiments, we varied σ between .01 and .001, set by cross validation. We used a fixed number of $R = 500$ reference points and observed consistent behavior at both double and half that amount. Given a fixed $\operatorname{Dist}_{\text{Global}}$, we can compute $w_{ij} = w_j(\mathbf{x}_i)$. Interpreting these values as the probability that training point \mathbf{x}_i selects metric $M_{RP}^{\mathbf{x}_{RP}^j}$, we can learn each $M_{RP}^{\mathbf{x}_{RP}^j}$ so as to minimize expected loss by optimizing Equation (LDA) and (LMNN) with weights w_{ij} . One could define a weighted version of Equation (8) that simultaneously learns all reference metrics. Since this involves a sum over the cross product of all imposter triples with all reference points, we chose not to do this.

We found empirically at first that the smooth weighted average metric in Equation (14) significantly outperformed the nearest neighbor algorithm. The computational cost of computing the smooth weighted average metric in Equation (14) is significantly more, however. Subsequently we found a different way of training the metrics at the reference points that largely eliminates this difference in performance. We now describe this approach.

We hypothesized that the smooth interpolation outperformed NN interpolation because the smoothing acted as an additional regularizer. To achieve the same regularization effect for NN interpolation, we applied a cross-validation step to construct a regularized version of $M_{RP}^{\mathbf{x}_{RP_i}}$:

$$M_{CV}^{\mathbf{x}_{RP_j}} = \frac{1}{Z_j} \sum_{i \neq j} w_i(\mathbf{x}) M_{RP}^{\mathbf{x}_{RP_i}} \quad (16)$$

where Z_j is a normalization factor included to ensure the sum of weights $w_i(\mathbf{x})$ for $j \neq i$ is 1, and $w_i(\mathbf{x})$ is defined as in Equation (15). $M_{CV}^{\mathbf{x}_{RP_i}}$ is equivalent to the metric tensor computed at $\mathbf{x} = \mathbf{x}_{RP_i}$ using Equation (14) but limiting the summation to include only the $R - 1$ other reference points. We found $MT_{NN}(\mathbf{x})$ computed with the above cross-validated metrics performed similarly to $MT_{RBF}(\mathbf{x})$, but was significantly faster. As such, our interpolation results reported in our experiments are generated with NN interpolation with $M_{CV}^{\mathbf{x}_{RP_j}}$.

So far we have described the interpolation of the reference point metrics for the test point \mathbf{x} . The same interpolation could be performed anywhere in the feature space. For example, it could be performed at the training points \mathbf{x}_i . This leads to a space-efficient version of Per-Exemplar. Another use of the interpolation algorithm is to compute the Line Integral of the metric tensor between the train and test points. We now describe this algorithm.

E. New Algorithms: Integration Along the Line Between Train and Test Points

Computing the geodesic distance in Equation (3) in high dimensions is intractable. In 2D or 3D the space can be discretized into a regular grid of vertices (pixels/voxels) and then either an (approximate) distance transform or a shortest path algorithm used to estimate the geodesic distance. In higher dimensions, however, discretizing the space yields a combinatorial explosion in the number of vertices to be considered. To avoid this problem, all of the above algorithms assume that the metric tensor is locally (or globally) constant and so can approximate the geodesic distance with the simple metric distance in Equation (1).

One way to obtain a better approximation of the geodesic is to assume that the space is not curved locally and approximate the minimum in Equation (3) with the integral along the line between the test point \mathbf{x} and the training point \mathbf{x}_i :

$$\mathbf{c}(\lambda) = \mathbf{x} + \lambda(\mathbf{x}_i - \mathbf{x}). \quad (17)$$

Substituting Equation (17) into Equation (2) and simplifying yields the **Line Integral** distance:

$$\text{Dist}_{\text{Line}}(\mathbf{x}, \mathbf{x}_i) = (\mathbf{x}_i - \mathbf{x})^T \left[\int_0^1 MT(\mathbf{c}(\lambda)) d\lambda \right] (\mathbf{x}_i - \mathbf{x}). \quad (18)$$

Note that the line distance is an upper bound on the geodesic distance:

$$\text{Dist}_{\text{Geo}}(\mathbf{x}, \mathbf{x}_i) \leq \text{Dist}_{\text{Line}}(\mathbf{x}, \mathbf{x}_i). \quad (19)$$

We now present a polynomial time algorithm to estimate the integral in Equation (18) *exactly* under the assumption that the metric tensor is piecewise constant, and using the nearest-neighbor interpolation algorithm in Section II-D.3.

We assume that the metric tensor has been sampled at the reference points to estimate $M_{RP}^{\mathbf{x}_{RP_i}}$. We also assume that the metric tensor is piecewise constant and its value at any given point \mathbf{x} is the value at the reference point which is closest, as measured by that reference points metric:

$$MT(\mathbf{x}) = M_{RP}^{\mathbf{x}_{RP_i}} \quad (20)$$

where for all $j = 1, \dots, R$:

$$(\mathbf{x} - \mathbf{x}_{RP_i})^T M_{RP}^{\mathbf{x}_{RP_i}} (\mathbf{x} - \mathbf{x}_{RP_i}) \leq (\mathbf{x} - \mathbf{x}_{RP_j})^T M_{RP}^{\mathbf{x}_{RP_j}} (\mathbf{x} - \mathbf{x}_{RP_j}). \quad (21)$$

Equation (21) divides the space into an “anisotropic Voronoi diagram” similarly to [25]. See Figure 3(right) for an illustration. The Voronoi diagram is anisotropic because the metric is different in each cell, whereas for a regular Voronoi diagram there is a single global metric. Equation (21) defines $R(R - 1)/2$ boundary surfaces, one between each pair of references points. There could, however, be an exponential number of cells as the addition of each new boundary surface could divide all of the others into two or more sub-cells.

To compute the integral in Equation (18) we need to break the domain $\lambda \in [0, 1]$ into the segments for which it is constant. The boundaries of the regions in Equation (21) are defined by the equalities:

$$(\mathbf{x} - \mathbf{x}_{RP_i})^T M_{RP}^{\mathbf{x}_{RP_i}} (\mathbf{x} - \mathbf{x}_{RP_i}) = (\mathbf{x} - \mathbf{x}_{RP_j})^T M_{RP}^{\mathbf{x}_{RP_j}} (\mathbf{x} - \mathbf{x}_{RP_j}). \quad (22)$$

Equation (22) is a quadratic and in general the solution is a quadratic hyper-surface. The intersection of this boundary hypersurface and the line between the test and training points in Equation (18) can be computed by substituting Equation (18) into Equation (22). The result

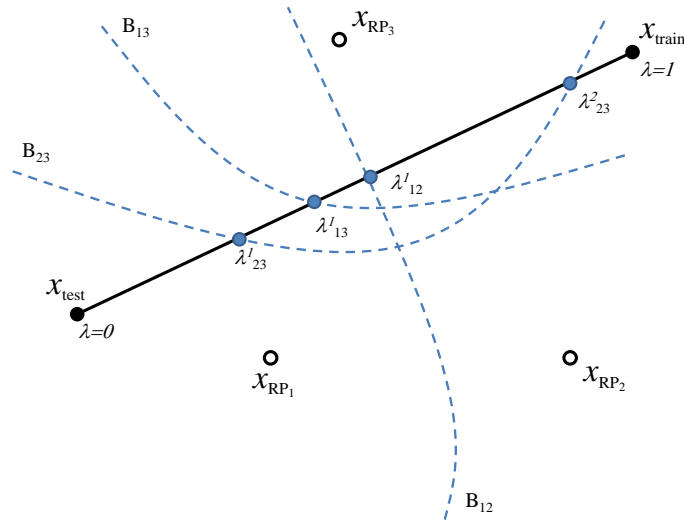


Fig. 4. An illustration of the computation of the exact polynomial integration of the metric tensor along the line from the training point to the test point under the assumption that the metric tensor is piecewise constant. In this example there are three reference points \mathbf{x}_{RP_1} , \mathbf{x}_{RP_2} , and \mathbf{x}_{RP_3} . The regions in space where the metric tensor is constant are bounded by quadratic hypersurfaces, in this case denoted B_{12} , B_{23} , and B_{13} . The intersection of these hypersurfaces and the line between the test point \mathbf{x}_{test} and the training point $\mathbf{x}_{\text{train}}$ can be computed by solving a quadratic in the single unknown λ . The solutions for λ that lie in the interval $[0, 1]$ can be sorted and then the integral approximated by adding up the length of the results segments, after searching for the appropriate reference point to use for each segment.

is a quadratic in the single unknown λ which can be solved to give either 0, 1 or 2 solutions in the range $[0, 1]$.

Once all the solutions that lie in $\lambda \in [0, 1]$ have been computed, they can be sorted. This breaks the line in Equation (18) into a number of segments where the metric tensor is constant on each one. The appropriate value of the metric tensor is then computed for each such segment by taking the midpoint of the segment and computing the closest reference point using Equation (21). The lengths of all the segments can then be computed and added up. In total, there can be at most $2R(R-1)/2$ intersection points. Computing each one takes time $O(K^2)$. There are at most $1 + R(R-1)$ segments of the line between the test and training points. The search for the closest reference point for each one takes $O(RK^2)$ because there are R reference points and the cost of computing the distance to it is $O(K^2)$. The total computation cost is therefore polynomial

$O(R^3 K^2)$.

III. EXPERIMENTS

We now present our experimental results. We describe the databases and how we sample them in Section III-A. We also describe two implementation details. In Section III-A.1 we describe candidate pruning. In Section III-A.2 we describe indexing structures. We describe the evaluation metrics and the result in Section III-B. We include some of the results in the Appendix, in tabular form following the taxonomy outlined in Figure I. The complete set of results are included in the online supplemental material at the author's website. In Section III-C we analyze the results in detail, plotting various interesting subsets.

A. Databases and Data Sampling

We compared the various algorithms on a diverse set of problems, including face recognition using MultiPIE [18], object recognition using Caltech 101 [11], and digit recognition using MNIST [27]. In Figure 5 we include a number of example images from each of the 3 databases.

MultiPIE [18] is a larger version of the CMU PIE database [36] that includes over 700,000 images of over 330 subjects collected in four sessions over six months. We extract the face regions automatically in the five frontal-most cameras (-45 degrees to +45 degrees) using the Viola-Jones face detector [41]. The face regions were then resampled and normalized to 80×80 grayscale patches with zero mean and unit variance. The patches were then projected into their first 254 principle components (95% of the empirical variance.) Different sessions were used as training and testing data. We randomly generated 10 batches of 1000 examples as our test sets.

Caltech 101 [11] is a widely used benchmark for image classification consisting of over 9,000 images from 101 object categories. We base our results on the widely-used single-cue baseline of spatial pyramid kernels [26]. We use the publicly available feature computation code from the author's website, which generates a sparse feature vector of visual word histograms for each image. We project the vectors such that 95% of the variance is captured, and then use them in our local distance function framework. We follow the established protocol of leave-one-out cross validation with 30 training examples per class. Using the online implementation provided by the author, we obtained an average classification rate of 62.18, slightly below the reported

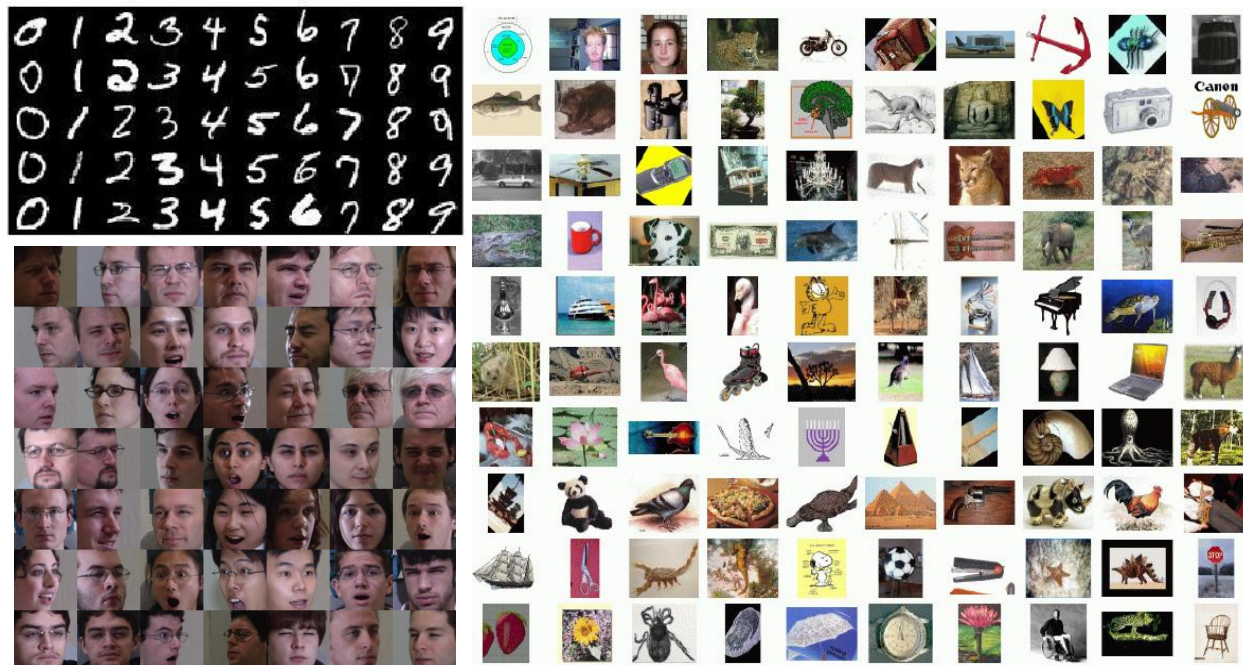


Fig. 5. Example images extracted from the 3 databases that we used. Bottom Left: MultiPIE [18]. Right: Caltech 101 [11]. Top Left: MNIST [27].

value of 64.6. Recent work exploiting multiple cues has improved this score [6], [21], [40], but we restrict ourselves to this established baseline for our analysis.

MNIST [27] is a well-studied dataset of 70,000 examples of digit images. We followed the pre-processing steps outlined by [24]. The original 28×28 dimensional images were deskewed and projected into their leading 164 principle components which were enough to capture 95% of the data variance. The normal MNIST train/test split [27] has two problems. (1) The training data is very dense with error rates around 1-2% making it hard to see any difference in performance. (2) There is only one partition making it impossible to estimate confidence intervals. To rectify these problems, we sub-sampled both the train and test data, in 10 batches of 1000 examples.

1) *Candidate Pruning*: Many of the algorithms in our taxonomy, though polynomial in space and time, can still be computationally demanding. In all cases we apply a short-listing approach similar to that used in previous work [3], [19], [43]. We first prune the large set of all candidate matches (the training points) with a global metric. In Figure 6 we consider the effect of varying the pruning threshold for three algorithms on the MultiPIE experiments. We find the recognition

performance of our algorithms to be stable over a large range. Based on this observation, we use a constant pruning threshold of 20 candidates. These 20 candidates are then matched to the test point using the various local algorithms.

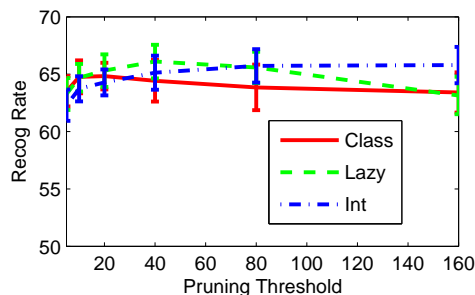


Fig. 6. We consider the effect of varying the pruning threshold on our evaluation methodology. We plot the recognition rate obtained by Per-Class, Lazy, and the Interpolation algorithm (using NN interpolation with cross-validated reference metrics, as described in Section II-D.3) for several different thresholds on the MultiPIE dataset. The recognition rate achieved by all three algorithms is relatively stable for a wide range of thresholds. For large pruning thresholds, the Lazy algorithm performs similar to a single Global metric since the local metric is learned from a large set of neighbors. The best performance is obtained by pruning to 20-40 candidates. Because a shorter pruned list results in an overall speedup across all algorithms that we consider, we fix the pruning threshold to 20 candidates in all experiments. Interpolation algorithms maybe even more competitive for larger pruning thresholds.

2) *Indexing Structures*: The pruning strategy just described above means that our algorithms generally require two nearest-neighbor searches. The first search generates the short list of candidates, while the second re-ranks the candidates to compute the final K-NN label. For low to mid dimensional data, KD trees [8] and other indexing structures based on randomized hashing [20] are known to be effective and enable fast search. Kulis, Jain, and Grauman describe methods of fast search for learned global metrics [22]. In Figure 7 (left), we show that the relative performance of the algorithms is unaffected by the use of a KD tree. In Figure 7 (right) we show that the use of such a structure can dramatically reduce the computation time, although the effect is less for online algorithms such as “Test” that learn the metric during the classification phase. The practical approach is therefore to use an indexing structure such as a KD tree for the first search and a brute-force search for the second search (where building a index structure would be more difficult or impossible due to the varying metrics that in some cases are only available online at classification time.) The development of efficient indexing structures specially tuned for local distance functions is left as an area for future work.

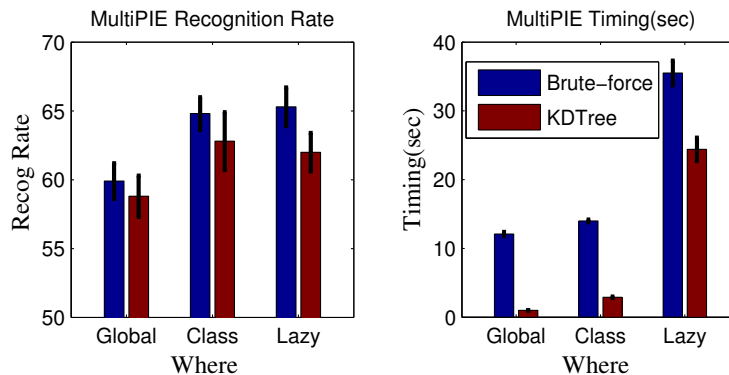


Fig. 7. We consider the effect of efficient indexing structures on our evaluation methodology. Using the MultiPIE dataset, we compare algorithms that vary along the “Where” dimension using a brute-force NN search versus a KD-tree based search. The KD-tree is only used during the initial candidate pruning stage. As shown above, algorithms whose computationally requirements are focused on the initial stage – such as Global or Per-Class – can see a significant speed up at the cost of a small decrease in performance. However, some of the algorithms we consider spend more computational effort on the second stage of re-ranking, making the efficiency of the initial indexing less prominent in the total computation time. An example is the Lazy algorithm that learns a metric at test-time. For simplicity, we present all timing results using a brute-force linear scan across all our experiments.

B. Evaluation Measures and Results

We obtain a final classification for each algorithm by applying K-NN with $K = 3$ on the re-ranked shortlisted neighbors of a test point. We computed a variety of evaluation measures. In particular, we computed (1) recognition rates, (2) error rates, (3) percentage reduction in the error rate from the global baseline, and (4) computation times. For each measure, we computed both the average values and the standard deviations across the sets of test samples (10 for MultiPIE and MNIST, and 30 for Caltech 101.) In the appendix we include a set of tables containing all of the recognition rate and computation time results. We include the full set of results for all four measures of performance in a set of interactive webpages in the online supplemental material.

C. Analysis of the Results

We now discuss the results in the context of our taxonomy of local distance functions. The criteria we consider for evaluation are both accuracy and computational cost. We perform a greedy exploration of our taxonomy, iteratively exploring dimensions given the best performing algorithm encountered thus far.

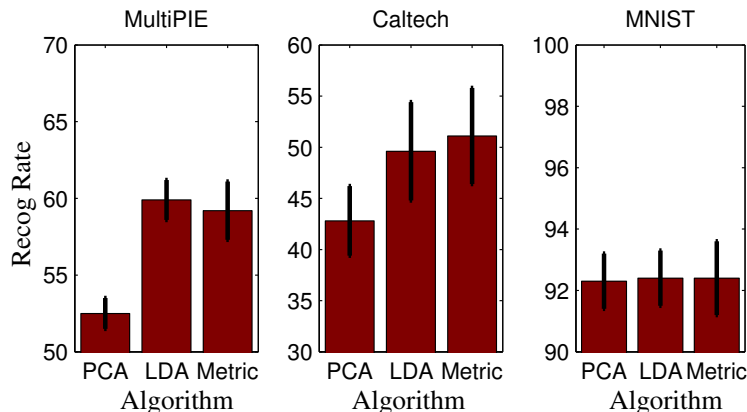


Fig. 8. A comparison of the global metrics. We find that LDA is competitive with more sophisticated approaches such as LMNN-based metric learning [24]. Our other experiments (see below) suggest that regularization is a key issue for metric learning. We hypothesize that LDA is competitive because it is easier to regularize than more sophisticated metric-learning approaches.

1) *Global*: We begin by examining the performance of the global metrics in Figure 8. We make a number of observations. First, metric learning tends to outperform simpler approaches such as PCA. Secondly, LDA-based metric learning is competitive with more recent and sophisticated approaches such as LMNN [24]. We hypothesize that this may be due to overfitting, and discuss this further below. Third, the various global metrics perform similarly on MNIST. The MNIST training data is relatively dense. As the training data gets more dense we expect to see less difference between the various metrics. However, we do see improvements using local distance functions (see below).

2) *Where*: Given the success of LDA in Figure 8, for the moment we fix our metric-learning algorithm to LDA and examine the “where” dimension of our taxonomy. We revisit this choice in Section III-C.3. The results in Figure 9 show that Per-Class metrics consistently outperform Global metrics across all three datasets. The relative performance increase across MultiPIE, Caltech, and MNIST is 8%, 10%, and 1% respectively. The large improvement in Caltech is likely due to the large inter-class variation, which is better captured by class-specific metrics. Our results are consistent with recent results in the metric-learning literature [4], [24], [40]. Interestingly, “per-exemplar” metrics tend to do worse than per-class, with the notable exception of Caltech. We believe that Caltech also contains a significant amount of intra-class variation –

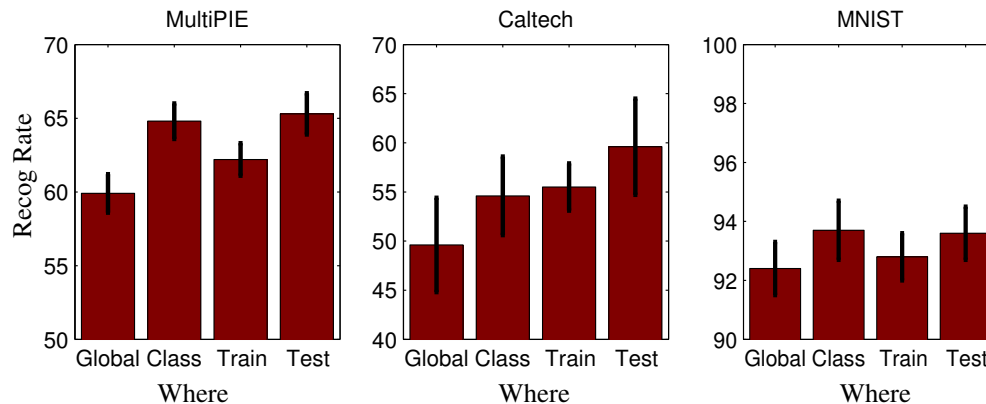


Fig. 9. Results across the “where” dimension of our taxonomy using LDA-based metric learning. We see that per-exemplar (Train) does not always outperform per-class even though it is a strictly more flexible model. We hypothesize two reasons. First, per-exemplar requires many more metrics and so tends to overfit the large number of parameters to be estimated. Second, it is difficult to ensure the multiple metrics are normalized appropriately so that distances computed using them are fairly comparable. The latter point is not an issue when a single metric is used centered at the test point, equivalent to classic “Lazy” approaches to learning [3], [19]. For LDA-based metric learning, the Lazy approach performed the best for all three datasets.

at least relative to our other datasets – and that this variation is better modeled by exemplar-specific metrics. However in general, we find that it is difficult to learn accurate per-exemplar metrics for the two following reasons. First, per-exemplar metric learning estimates many more metrics and so suffers from over-fitting due to the large number of parameters to be learned. Secondly, it is difficult to ensure that multiple metrics are appropriately normalized so that the distances computed using them are comparable. The second of these shortcomings are dealt with by directly learning a metric at the Test point. Our experimental results in Figure 8 suggest that such classic Lazy algorithms [3], [19] are competitive with, or even outperform, more recent “per-class” and “per-exemplar” approaches for local metric learning. We show an example of the Lazy algorithm in Figure 10.

3) *How*: Given the success of the Lazy algorithm in Figure 12, we focus on the Lazy algorithm and re-examine the choice of the metric-learning algorithm. In Figure 11 we include results for the “How” dimension of our taxonomy. We find that LMNN noticeably under-performs LDA-based metric learning in the Lazy setting. We hypothesize this is the case because the second-stage metric is learned from a small set of shortlisted neighbors. Discriminative learning approaches such as LMNN are known to be more susceptible to overfitting [31]. LDA performs better with

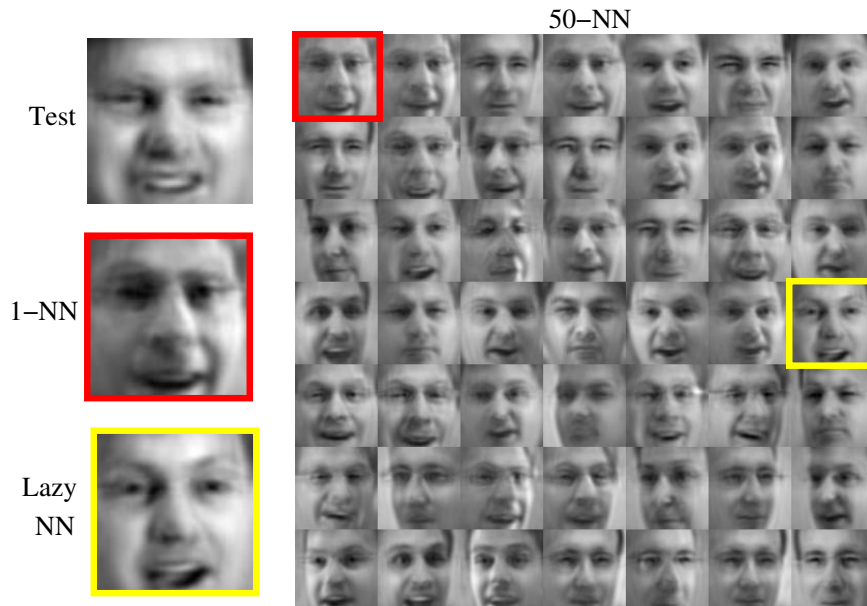


Fig. 10. Why does Lazy local metric-learning work well? We consider an example from the MultiPIE database. We show a test image and its 50-NN, ordered by distance, under a global LDA metric. The 50-NN tend to have the same expression and pose as the test point. However, the 1-NN happens to be incorrectly labeled. A local metric computed from these 50-NN will be tailored to this specific expression and pose. This is in contrast to both a global and class-specific metric which must attempt to be invariant to these factors. This makes the Lazy local metric better suited for disambiguating classes near this test point. We show the correctly classified NN using the Lazy metric in the **bottom left**.

less training data because of its underlying generative modeling assumptions and because it is straightforward to regularize. Our novel hybrid algorithm exploits the strengths of each approach, using LMNN for the initial global search where more training data is available, and LDA for local metric-learning where training data is sparse.

4) *When:* Our experimental analysis to this point suggests that the Hybrid Lazy algorithm performs the best. One drawback of Lazy learning is its run-time cost. For certain applications, this may be impractical. We examine tradeoffs between recognition rate and run-time in Figure 12. Comparing the best off-line approach (Per-class) with the best on-line approach (Lazy), we see that Lazy tends to perform better but can be orders of magnitude slower. This is especially true of LMNN-based metric-learning, which requires solving a semi-definite program (SDP) for each test point. Our novel interpolation algorithm shifts the metric learning computation offline, only requiring online interpolation. Interpolated metrics, while not performing as well as Lazy

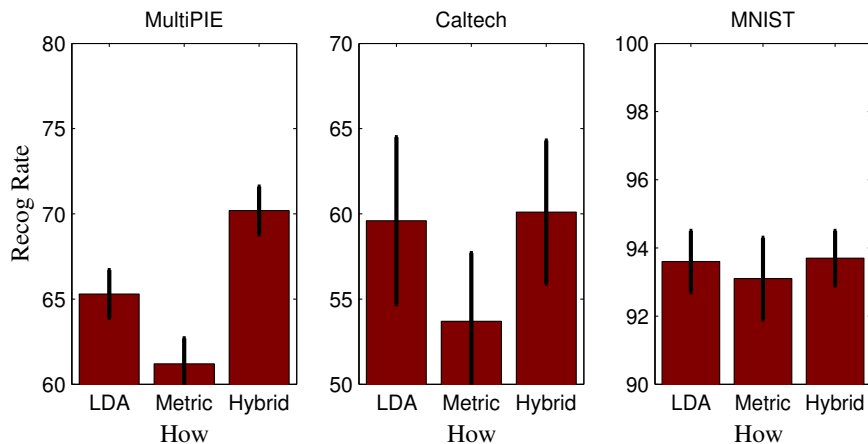


Fig. 11. Results across the “how” dimension of our taxonomy for the Lazy algorithm. Lazy requires two metrics - one to produce an initial short list of neighbors, and a second used to rerank the candidates in the short list. We show that a hybrid approach which uses LMNN for the first stage and LDA for the second works the best. We hypothesize that this is the case because discriminative metric-learning suffers less from overfitting in the global regime, where plenty of data is available. LDA performs better when learning metrics from a smaller set of local data because LDA is easier to regularize and enjoys some resistance to overfitting due its underlying generative nature [31].

metrics, are considerably faster. Note that for metric-learning, the interpolated metrics generally perform better than the Lazy algorithm. A likely explanation is that as interpolation provides additional regularization.

5) *Line Integral*: We now revisit the “where” dimension of our taxonomy, focusing on our novel line-integral algorithm under our novel hybrid learning scheme. See Figure 13 for the results. We make two observations. In hybrid learning, per-exemplar metrics are competitive with per-class metrics, presumably due to the increased regularization from local LDA. Secondly, our Line Integral algorithm, while clearly outperforming the global baseline, does not do as well as Lazy. Consider a simplified scenario in which the line connecting a test and training point only passed through two metrics centered at those two points. In this case, the line integral distance would be a weighted average of the distances computed by the Per-Exemplar and Lazy algorithms. Our results show that the integral distance performs worse than either of those algorithms. Empirically we find that the line passes through many more metrics, and we hypothesize that these additional metrics are polluting the weighted average computed by the algorithm. While this is a negative result and therefore primarily of theoretical interest, it is

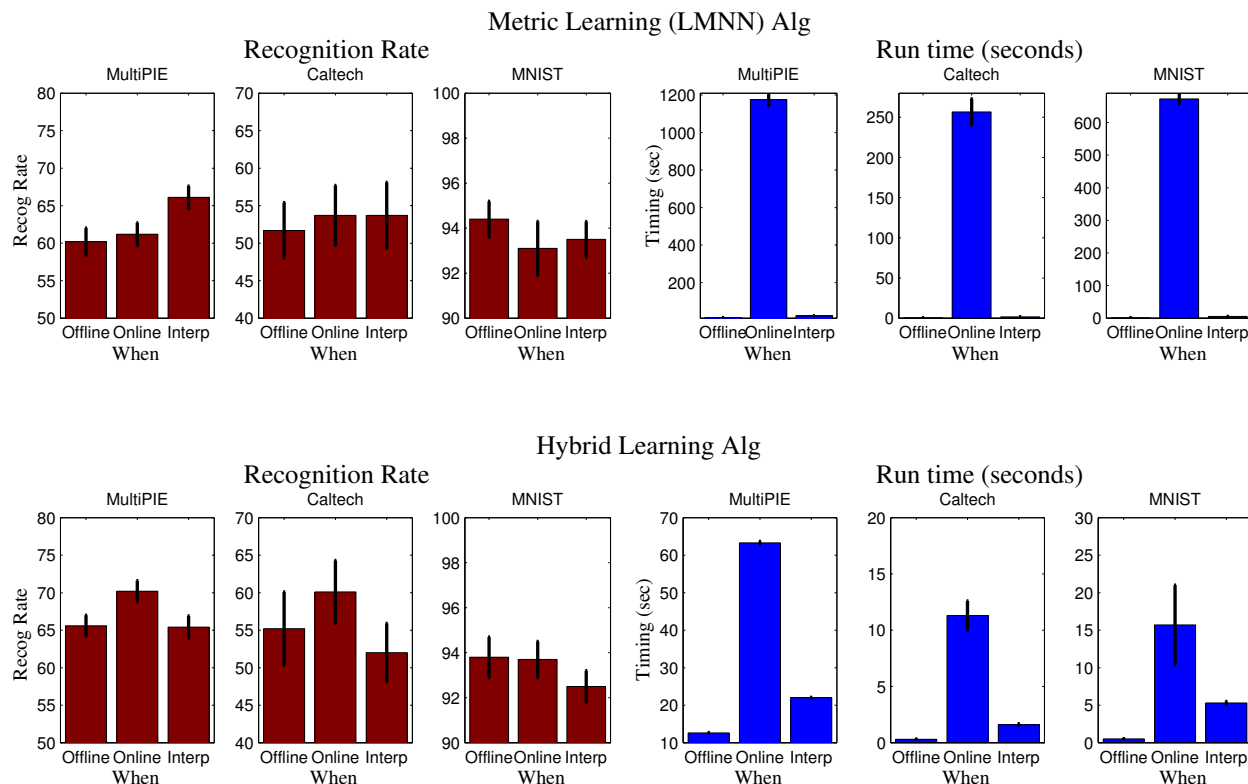


Fig. 12. Results for the “when” dimension of our taxonomy for both metric-learning (**top**) and our hybrid algorithm (**bottom**). On the **left** we show recognition rates, while on the **right** we show run-times for classification. In the above graphs “off-line” refers to Per-class metric learning, which we generally find to be a good choice for off-line metric learning. We write “on-line” to refer to the Lazy algorithm that estimates the metric at the test point. We show results for our novel “interpolation” algorithm that approximates Lazy while still shifting computation off-line. In LMNN metric-learning, interpolation tends to outperform the on-line Lazy algorithm, probably due to increased regularization. In Hybrid learning, where overfitting is less of an issue, interpolated metrics perform similarly to, or slightly worse than, their Lazy counterparts. Interpolated metrics are significantly faster in either case, and dramatically so for Metric Learning. We attribute the success of the off-line algorithm in MNIST to its lack of intra-class variation (eliminating the need for a more flexible “on-line” Lazy metric estimation).

still important to show that little can be gained by such an approach.

6) *Previous Reported Results:* Our MultiPIE results are comparable to those reported in [18], but are obtained automatically without manually marked fiducial locations. Our score of 60.1 on Caltech is comparable to the score of 62.2 we obtained by running the author’s code from [26], which itself is slightly below the reported value of 64.6. We hypothesize the chi-squared kernel from [26] performs a form of local weighting. Our MNIST results are not directly comparable to previous work because we use subsampled data, but our class-specific learned-metric baseline

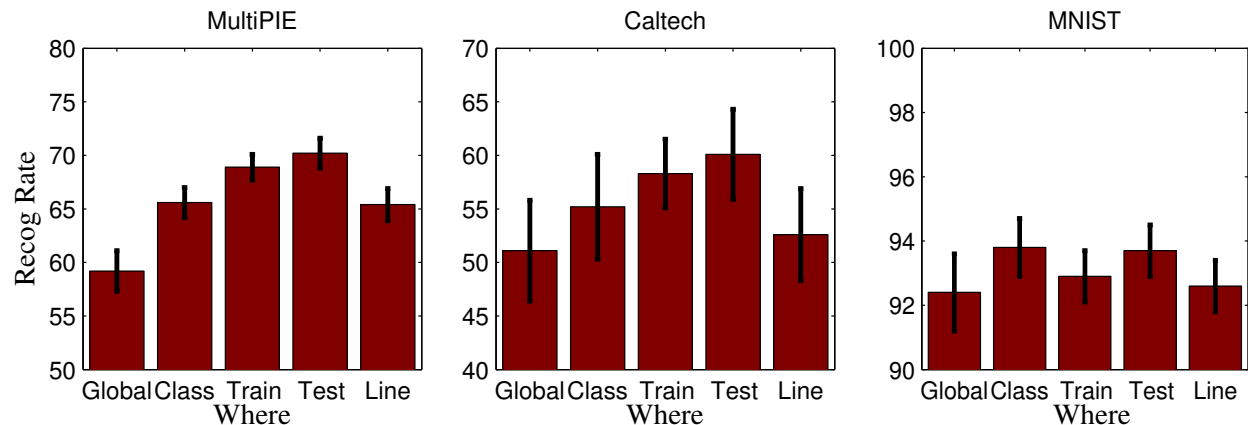


Fig. 13. We revisit the “where” dimension of our taxonomy using our hybrid algorithm, including results for our novel Line integral algorithm. While the Line integral approach consistently outperforms a single Global metric, it is outperformed by simpler approaches such as per-class and Lazy. We hence view this algorithm as primarily of theoretical interest.

produces the state-of-the-art MNIST results on the full train/test split [24]. We verified that the author’s code reproduced the reported results, and ran the same code on random train/test splits. Overall, though our benchmark results do not always advance the state-of-the-art, our evaluation clearly reveals the benefit of local approaches over global baselines.

IV. CONCLUSION

We have presented a taxonomy of local distance functions in terms of **how**, **where**, and **when** they estimate the metric tensor and approximate the geodesic distance. We have extended this taxonomy along all three axis. We performed a thorough evaluation of the full combination of algorithms on three large scale, diverse datasets. Overall, the main conclusions are that the Hybrid, Lazy estimation of the metric at the test point performs the best. One issue with the Hybrid, Lazy algorithm is the computational cost. If high efficiency is vital, the Interpolation version of the Lazy algorithm and the Per-Class algorithm provide good alternatives, with Per-Class consistently outperforming Interpolation for hybrid metric-learning.

Overall, we found the generalization ability of the learned metrics to be a recurring key issue. Local metrics are learned using a small subset of the training data, and so overfitting is a fundamental difficulty. As a result, regularized LDA was often competitive with LMNN. We obtained good results when using LMNN to train a global model but found LDA was generally

better at estimating the local metrics (especially in the hybrid algorithm.)

A. Future work

We see interesting future directions both in terms of improving the recognition rate and in terms of reducing the computational cost. One possible direction is to extend our taxonomy to kernel-based NN classification, eliminating the requirement for a finite dimensional vector-space embedding of data. Casting such a formulation in a SVM-based hinge-loss framework, it might be possible to improve the run-time speed by only matching to a sparse set of support training examples. Recent work [4] has suggested an addition to the “Where” dimension of our taxonomy by assuming that groups of classes share the same metric. Such an approach has the potential to reduce overfitting. Finally, another possible direction is to extend efficient indexing structures, such as KD trees, to local metrics.

ACKNOWLEDGMENTS

We thank Killian Weinberger for providing the code for Large Margin Nearest Neighbors (LMNN) [24] and Svetlana Lazebnik for providing the code for spatial pyramid kernels [26].

REFERENCES

- [1] http://en.wikipedia.org/wiki/Metric_tensor.
- [2] <http://mathworld.wolfram.com/MetricTensor.html>.
- [3] C. Atkeson, A. Moore, and S. Schaal. Locally weighted learning. *Artificial Intelligence Review*, 11:11–73, 1997.
- [4] B. Babenko, S. Branson, and S. Belongie. Similarity Metrics for Categorization: From Monolithic to Category Specific. In *Proceedings of the IEEE International Conference on Computer Vision*, 2009.
- [5] A. Bar-Hillel, T. Hertz, N. Shental, and D. Weinshall. Learning and mahalanobis metric from equivalence constraints. *Journal of Machine Learning Research*, 6:937–965, 2005.
- [6] O. Boiman, E. Shechtman, and M. Irani. In defense of nearest-neighbor based image classification. In *Proceedings of the IEEE Conference on Computer Vision and Pattern Recognition*, 2008.
- [7] D. Broomhead and D. Lowe. Radial basis functions, multi-variable functional interpolation and adaptive networks, 1988.
- [8] T. Cormen, C. Leiserson, R. Rivest, and C. Stein. *Introduction to algorithms*. MIT Press, 2001.
- [9] N. Cristianini and J. Shawe-Taylor. *An introduction to support Vector Machines: and other kernel-based learning methods*. Cambridge University Press, 2000.
- [10] C. Domeniconi, J. Peng, and D. Gunopulos. Locally adaptive metric nearest-neighbor classification. *IEEE Transactions on Pattern Analysis and Machine Intelligence*, 24(9):1281–1285, 2002.
- [11] L. Fei-Fei, R. Fergus, and P. Perona. Learning generative visual models from few training examples: an incremental bayesian approach tested on 101 object categories. In *Proceedings of the IEEE Conference on Computer Vision and Pattern Recognition, Workshop on Generative-Model Based Vision*, 2004.

- [12] A. Frome, Y. Singer, and J. Malik. Image retrieval and classification using local distance functions. *Advances in Neural Information Processing Systems*, 19:417–424, 2007.
- [13] A. Frome, Y. Singer, F. Sha, and J. Malik. Learning globally-consistent local distance functions for shape-based image retrieval and classification. In *Proceedings of the IEEE International Conference on Computer Vision*, 2007.
- [14] K. Fukunaga. *Introduction to Statistical Pattern Recognition*. Academic Press, 1990.
- [15] J. Goldberger, S. Roweis, and R. Salakhutdinov. Neighborhood components analysis. *Advances in Neural Information Processing Systems*, 17:513–520, 2005.
- [16] M. Gonen and E. Alpaydin. Localized multiple kernel learning. In *Proceedings of the International Conference on Machine Learning*, 2008.
- [17] K. Grauman and T. Darrell. Efficient learning with sets of features. *Journal of Machine Learning Research*, 8:725–760, 2007.
- [18] R. Gross, I. Matthews, J. Cohn, T. Kanade, and S. Baker. Multi-PIE. In *Proceedings of the IEEE International Conference on Automatic Face and Gesture Recognition*, 2008.
- [19] T. Hastie and R. Tibshirani. Discriminant adaptive nearest neighbor classification. *IEEE Transactions on Pattern Analysis and Machine Intelligence*, 18(6):607–616, 1996.
- [20] P. Indyk and R. Motwani. Approximate nearest neighbors: towards removing the curse of dimensionality. In *Proceedings of the thirtieth annual ACM symposium on Theory of computing*, pages 604–613, 1998.
- [21] A. Kapoor, K. Grauman, R. Urtasun, and T. Darrell. Gaussian processes for object categorization. *International Journal of Computer Vision*, 2009. To appear.
- [22] B. Kulis, P. Jain, and K. Grauman. Fast Similarity Search for Learned Metrics. *IEEE Transactions on Pattern Analysis and Machine Intelligence*, 31(12):2143, 2009.
- [23] M. Kumar, P. Torr, and A. Zisserman. An invariant large margin nearest neighbour classifier. In *Proceedings of the IEEE International Conference on Computer Vision*, 2007.
- [24] K. Weinberger and L. Saul. Distance metric learning for large margin nearest neighbor classification. *Journal of Machine Learning Research*, 2009. To appear.
- [25] F. Labelle and J. Shewchuk. Anisotropic voronoi diagrams and guaranteed-quality anisotropic mesh generation. In *Proceedings of the 19th Annual Symposium on Computational Geometry*, pages 191–200, 2003.
- [26] S. Lazebnik, C. Schmid, and J. Ponce. Beyond bags of features: Spatial pyramid matching for recognizing natural scene categories. In *Proceedings of the IEEE Conference on Computer Vision and Pattern Recognition*, volume 2, pages 2169–2178, 2006.
- [27] Y. Lecun, L. Bottou, Y. Bengio, and P. Haffner. Gradient-based learning applied to document recognition. *Proceedings of the IEEE*, 86(11):2278–2324, 1998.
- [28] S. Mahamud and M. Hebert. The optimal distance measure for object detection. In *Proceedings of the IEEE Conference on Computer Vision and Pattern Recognition*, volume 1, pages 248–255, 2003.
- [29] S. Maji and A. Berg. Max-margin Additive Classifiers for Detection. In *Proceedings of the IEEE International Conference on Computer Vision*, 2009.
- [30] T. Malisiewicz and A. Efros. Recognition by association via learning per-exemplar distances. In *Proceedings of the IEEE Conference on Computer Vision and Pattern Recognition*, 2008.
- [31] A. Ng and M. Jordan. On discriminative vs. generative classifiers: A comparison of logistic regression and naive bayes. *Advances in Neural Information Processing Systems*, 14:841–848, 2002.
- [32] D. Ramanan and S. Baker. Local Distance Functions: A Taxonomy, New Algorithms, and an Evaluation. In *Proceedings of the IEEE International Conference on Computer Vision*, 2009.

- [33] R. Rifkin and A. Klautau. In defense of one-vs-all classification. *The Journal of Machine Learning Research*, 5:101–141, 2004.
- [34] E. Rosch and C. Mervis. Family resemblances: Studies in the internal structure of categories. *Cognitive Psychology*, 7:573–605, 1975.
- [35] G. Shakhnarovich, P. Viola, and T. Darrell. Fast pose estimation with parameter-sensitive hashing. In *Proceedings of the IEEE International Conference on Computer Vision*, volume 1, pages 750–757, 2003.
- [36] T. Sim, S. Baker, and M. Bsat. The CMU Pose, Illumination, and Expression (PIE) Database. In *Proceedings of the IEEE International Conference on Automatic Face and Gesture Recognition*, 2002.
- [37] P. Simard, Y. LeCun, and J. Denker. Efficient pattern recognition using a new transformation distance. *Advances in Neural Information Processing Systems*, 5:50–58, 1993.
- [38] L. Torresani and K. Lee. Large margin component analysis. *Advances in Neural Information Processing Systems*, 19:1385–1392, 2007.
- [39] R. Urtasun and T. Darrell. Local probabilistic regression for activity-independent human pose inference. In *Proceedings of the IEEE Conference on Computer Vision and Pattern Recognition*, 2008.
- [40] M. Varma and D. Ray. Learning the discriminative power-invariance trade-off. In *Proceedings of the IEEE International Conference on Computer Vision*, 2007.
- [41] P. Viola and M. Jones. Rapid object detection using a boosted cascade of simple features. In *Proceedings of the IEEE Conference on Computer Vision and Pattern Recognition*, volume 1, pages 511–518, 2001.
- [42] X. Wang and X. Tang. Random sampling LDA for face recognition. In *Proceedings of the IEEE Conference on Computer Vision and Pattern Recognition*, volume 2, pages 259–265, 2004.
- [43] H. Zhang, A. Berg, M. Maire, and J. Malik. SVM-KNN: Discriminative nearest neighbor classification for visual category recognition. In *Proceedings of the IEEE Conference on Computer Vision and Pattern Recognition*, volume 2, pages 2126–2136, 2006.

APPENDIX

TABULATION OF RESULTS

In Tables II-IV we include all the recognition rate and computation time results. Table II includes results for LDA. Table III includes the results for LMNN. Table IV includes the results for the Hybrid algorithm. The full set of results, including the error rate and percentage reduction in the error rate results, are included in a set of interactive webpages in the supplemental material.

TABLE II

RECOGNITION RATE AND COMPUTATION TIME RESULTS FOR OUR TAXONOMY USING LDA-BASED METRIC-LEARNING. WE

DO NOT INCLUDE TIMING RESULTS FOR ONLINE/INTERPOLATED GLOBAL/CLASS METRICS BECAUSE AN OFFLINE IMPLEMENTATION IS MORE EFFICIENT. WE MARK THE BEST-PERFORMING ALGORITHM FOR EACH DATASET IN BOLD.

TEST-TIME METRIC ESTIMATION, OR LAZY LEARNING, TENDS TO DO WELL OVERALL, WHILE CLASS-BASED METRIC LEARNING SCORES marginally better in MNIST.

MultiPIE LDA Recognition Rate							Time (seconds)				
		Where					Where				
		Global	Class	Train	Test	Line	Global	Class	Train	Test	Line
When	Offline	59.9 ± 1.3	64.8 ± 1.2	N/A	N/A	N/A	5.0 ± 0.9	15.9 ± 2.5	N/A	N/A	N/A
	Online	59.9 ± 1.3	64.8 ± 1.2	62.2 ± 1.1	65.3 ± 1.4	N/A	-	-	1159 ± 173	59.0 ± 5.9	N/A
	Interp	59.9 ± 1.3	64.8 ± 1.2	64.3 ± 1.2	64.3 ± 1.1	64.4 ± 1.2	-	-	19.6 ± 3.4	28.3 ± 3.7	281.4 ± 40.0

Caltech LDA Recognition Rate							Time (seconds)				
		Where					Where				
		Global	Class	Train	Test	Line	Global	Class	Train	Test	Line
When	Offline	49.6 ± 4.8	54.6 ± 4.0	N/A	N/A	N/A	0.1 ± 0.1	0.3 ± 0.0	N/A	N/A	N/A
	Online	49.6 ± 4.8	54.6 ± 4.0	55.5 ± 2.4	59.6 ± 4.9	N/A	-	-	208.1 ± 12.9	10.9 ± 0.9	N/A
	Interp	49.6 ± 4.8	54.6 ± 4.0	51.6 ± 3.5	50.5 ± 3.4	51.4 ± 3.1	-	-	0.6 ± 0.1	1.4 ± 0.1	31.1 ± 3.1

Sampled MNIST LDA Recognition Rate							Time (seconds)				
		Where					Where				
		Global	Class	Train	Test	Line	Global	Class	Train	Test	Line
When	Offline	92.4 ± 0.9	93.7 ± 1.0	N/A	N/A	N/A	0.1 ± 0.0	0.6 ± 0.1	N/A	N/A	N/A
	Online	92.4 ± 0.9	93.7 ± 1.0	92.8 ± 0.8	93.6 ± 0.9	N/A	-	-	375.3 ± 19.1	19.5 ± 1.4	N/A
	Interp	92.4 ± 0.9	93.7 ± 1.0	92.7 ± 0.7	92.5 ± 0.7	92.6 ± 0.7	-	-	3.9 ± 0.5	7.2 ± 1.2	114.7 ± 8.4

TABLE III

RECOGNITION RATE AND COMPUTATION TIME RESULTS FOR ALL VARIANTS OF OUR TAXONOMY FOR THE METRIC-LEARNING APPROACH. TEST-TIME METRIC ESTIMATION, OR LAZY LEARNING, DOES NOT DO WELL BECAUSE METRIC-LEARNING TENDS TO OVERFIT. IN THIS CASE, AN ONLINE IMPLEMENTATION OF PER-EXEMPLAR TENDS TO PERFORM WELL, WHILE PER-CLASS AGAIN DOES WELL ON MNIST. WE SHOW THAT OUR HYBRID ALGORITHM OUTPERFORMS THESE RESULTS IN TABLE IV.

		MultiPIE Metric Learning Recognition Rate					Time (seconds)				
		Where					Where				
		Global	Class	Train	Test	Line	Global	Class	Train	Test	Line
When	Offline	59.2 ± 1.9	60.2 ± 1.8	N/A	N/A	N/A	3.6 ± 0.3	12.9 ± 0.6	N/A	N/A	N/A
	Online	59.2 ± 1.9	60.2 ± 1.8	68.8 ± 1.3	61.2 ± 1.5	N/A	-	-	1222 ± 9	1175 ± 32	N/A
	Interp	59.2 ± 1.9	60.2 ± 1.8	66.2 ± 1.5	66.1 ± 1.5	66.1 ± 1.6	-	-	14.6 ± 0.8	22.4 ± 0.9	184.6 ± 8.7

		Caltech Metric Learning Recognition Rate					Time (seconds)				
		Where					Where				
		Global	Class	Train	Test	Line	Global	Class	Train	Test	Line
When	Offline	51.1 ± 4.7	51.7 ± 3.7	N/A	N/A	N/A	0.1 ± 0.0	0.3 ± 0.0	N/A	N/A	N/A
	Online	51.1 ± 4.7	51.7 ± 3.7	58.2 ± 3.1	53.7 ± 4.0	N/A	-	-	222.4 ± 26.2	256.7 ± 16.3	N/A
	Interp	51.1 ± 4.7	51.7 ± 3.7	53.6 ± 4.4	53.7 ± 4.4	53.8 ± 4.5	-	-	0.8 ± 0.2	1.7 ± 0.1	39.9 ± 6.8

		Sampled MNIST Metric Learning Recognition Rate					Time (seconds)				
		Where					Where				
		Global	Class	Train	Test	Line	Global	Class	Train	Test	Line
When	Offline	92.4 ± 1.2	94.4 ± 0.8	N/A	N/A	N/A	0.1 ± 0.0	0.6 ± 0.0	N/A	N/A	N/A
	Online	92.4 ± 1.2	94.4 ± 0.8	92.8 ± 0.7	93.1 ± 1.2	N/A	-	-	310.2 ± 3.7	672.3 ± 15.4	N/A
	Interp	92.4 ± 1.2	94.4 ± 0.8	93.5 ± 0.8	93.5 ± 0.8	93.5 ± 0.8	-	-	3.0 ± 0.0	5.2 ± 0.1	98.1 ± 0.9

TABLE IV

RECOGNITION RATE AND COMPUTATION TIME RESULTS FOR ALL VARIANTS OF THE HYBRID ALGORITHM (SECTION II-B.3.) OVERALL, ONLINE ESTIMATION OF THE METRIC TENSOR AT THE TEST POINT IN OUR HYBRID FRAMEWORK TENDED TO PERFORM THE BEST ACROSS TABLES II-IV. PER-CLASS PERFORMED BEST FOR MNIST, CONSISTENT WITH PREVIOUS REPORTED RESULTS [24].

		MultiPIE Hybrid Recognition Rate					Time (seconds)				
		Where					Where				
		Global	Class	Train	Test	Line	Global	Class	Train	Test	Line
When	Offline	59.2 ± 1.9	65.6 ± 1.4	N/A	N/A	N/A	3.5 ± 0.0	12.6 ± 0.1	N/A	N/A	N/A
	Online	59.2 ± 1.9	65.6 ± 1.4	68.9 ± 1.2	70.2 ± 1.4	N/A	-	-	1219 ± 12	63.3 ± 0.4	N/A
	Interp	59.2 ± 1.9	65.6 ± 1.4	65.4 ± 1.5	65.4 ± 1.5	65.4 ± 1.5	-	-	14.3 ± 0.2	22.0 ± 0.1	184.5 ± 1.6

		Caltech Hybrid Recognition Rate					Time (seconds)				
		Where					Where				
		Global	Class	Train	Test	Line	Global	Class	Train	Test	Line
When	Offline	51.1 ± 4.7	55.2 ± 4.9	N/A	N/A	N/A	0.1 ± 0.0	0.3 ± 0.0	N/A	N/A	N/A
	Online	51.1 ± 4.7	55.2 ± 4.9	58.3 ± 3.2	60.1 ± 4.2	N/A	-	-	223.7 ± 29.0	11.3 ± 1.3	N/A
	Interp	51.1 ± 4.7	55.2 ± 4.9	53.0 ± 4.0	52.0 ± 3.9	52.6 ± 4.3	-	-	0.7 ± 0.0	1.6 ± 0.1	40.3 ± 6.9

		Sampled MNIST Hybrid Recognition Rate					Time (seconds)				
		Where					Where				
		Global	Class	Train	Test	Line	Global	Class	Train	Test	Line
When	Offline	92.4 ± 1.2	93.8 ± 0.9	N/A	N/A	N/A	0.1 ± 0.0	0.5 ± 0.0	N/A	N/A	N/A
	Online	92.4 ± 1.2	93.8 ± 0.9	92.9 ± 0.8	93.7 ± 0.8	N/A	-	-	311.1 ± 3.1	15.7 ± 0.5	N/A
	Interp	92.4 ± 1.2	93.8 ± 0.9	92.6 ± 0.7	92.5 ± 0.7	92.6 ± 0.8	-	-	3.1 ± 0.2	5.3 ± 0.2	97.8 ± 1.6